



Published in final edited form as:

Nat Genet. 2009 May ; 41(5): 524–526. doi:10.1038/ng.371.

Cooperativity of *TMPRSS2-ERG* with PI3-kinase pathway activation in prostate oncogenesis

Jennifer C. King¹, Jin Xu¹, John Wongvipat¹, Haley Hieronymus¹, Brett S. Carver¹, David H. Leung¹, Barry S. Taylor^{2,3}, Chris Sander², Robert D. Cardiff⁴, Suzana S. Couto⁵, William L. Gerald¹, and Charles L. Sawyers^{1,6}

¹Human Oncology and Pathogenesis Program, Memorial Sloan-Kettering Cancer Center, 1275 York Avenue, New York, NY 10065

²Computational and Systems Biology Center, Memorial Sloan-Kettering Cancer Center, 1275 York Avenue, New York, NY 10065

³Department of Physiology and Biophysics, Weill Medical College of Cornell University, New York, NY 10065

⁴Center for Comparative Medicine, Department of Pathology and Laboratory Medicine, University of California, Davis 95616

⁵Laboratory of Comparative Pathology, Memorial Sloan-Kettering Cancer Center, 1275 York Avenue, New York, NY 10065

⁶Howard Hughes Medical Institute, Memorial Sloan-Kettering Cancer Center, 1275 York Avenue, New York, NY 10065

Abstract

The *TMPRSS2-ERG* fusion, present in 50% of prostate cancers, is less common in prostatic intra-epithelial neoplasia (PIN), raising questions about whether *TMPRSS2-ERG* contributes to disease initiation. We identified the translational start site of a common *TMPRSS2-ERG* fusion and showed that transgenic *TMPRSS2-ERG* mice develop PIN, but only in the context of PI3-kinase pathway activation. *TMPRSS2-ERG* positive human tumors are also enriched for PTEN loss, suggesting cooperation in prostate tumorigenesis.

Recurrent gene fusions involving members of the ETS family of transcription factors occur frequently in human prostate cancer¹. The *TMPRSS2-ERG* fusion gene, generated by an intrachromosomal deletion on chromosome 21 or by reciprocal translocation, is the most common rearrangement, found in ~50% of localized tumors¹. The fusion is detected in essentially all the malignant cells within a focus of tumor, supporting a role in disease initiation. However, *TMPRSS2-ERG* is less commonly found in preneoplastic PIN lesions and, when present, is typically in PIN adjacent to fusion-positive tumor cells². Potential explanations for the relatively low frequency of *TMPRSS2-ERG* in PIN versus cancer are: (i) *TMPRSS2-ERG* is not an initiating event, (ii) PIN may not be a reliable precursor lesion to invasive cancer, or (iii) PIN is molecularly heterogeneous but *TMPRSS2-ERG* driven PIN progresses rapidly to cancer.

Author contributions

J.C.K., J.X., J.W., D.H.L., B.S.C. and C.L.S. designed, created, and characterized the transgenic animals. S.S.C. and R.D.C. provided the pathological analysis. J.X. and C.L.S. identified the potential start site. H.H., B.T., C.S., and W.L.G. performed and analyzed the CGH and exon array experiments. J.C.K. and C.L.S. wrote the initial draft of the manuscript and all authors contributed to the final version.

We addressed this question by generating transgenic mice expressing the *TMPRSS2-ERG* fusion in the prostate. Two *ERG* isoforms (variants 1 and 2) have been characterized, which differ in the N terminus as well as the presence of a downstream *ERG* exon due to alternative splicing. We designed our *TMPRSS2-ERG* construct (Fig. 1a) to re-create the most common translocation breakpoints³ and used the variant 2 *ERG* isoform based on exon array expression profiling data showing relative abundance of variant 2 in *TMPRSS2-ERG* positive human tumors⁴. Due to N-terminal truncation of *ERG* and fusion to non-coding *TMPRSS2* sequence, the initiating methionine for *ERG* translation is removed, raising questions about the translational start site of *TMPRSS2-ERG* fusion mRNA. To address this issue, we conducted mass spectrometry analysis of the protein product of our *TMPRSS2-ERG* fusion (Fig. 1c, lane 4) and recovered five tryptic peptides. The most N-terminal peptide spanned amino acids 58–70 of *ERG* (nucleotides 358–396), narrowing down the possible start codon to the methionine encoded by nucleotide 304 (Met 40 in full length *ERG*) or to Met 54 at nucleotide 356 (Fig. 1b). Mutation of the ATG encoding Met 40 to AAG substantially impaired translation of the *TMPRSS2-ERG* protein (Fig 1c, compare lanes 4 and 5) and, in the context of full length *ERG*, eliminated expression of the faster migrating *ERG* isoform observed with wild-type *ERG* overexpression (Fig. 1c, compare lanes 2 and 3). These data implicate Met 40 as the principle start site for *ERG* expression in the *TMPRSS2-ERG* fusion as well as a potential alternative start site for wild-type *ERG* expression.

To create transgenic mice, we placed the *TMPRSS2-ERG* fusion construct under the control of the *ARR2-Probasin* promoter, used in previous models of PIN and prostate cancer^{5–7}. Seventeen transgene-positive founder animals were generated by injection of the *ARR2-PB-TMPRSS2-ERG* construct into FVB blastocysts (Fig. 1d) and four demonstrated stable germline transmission of the transgene. Two lines (43 and 44) were expanded based on robust transgene expression at levels 20-fold greater than endogenous mouse *Erg* (Fig. 1e) and comparable to levels observed in an independently derived mouse expressing full length *ERG* variant 1⁸. Prostates from *TMPRSS2-ERG* fusion mice from both lines were harvested at 2, 6, 12 and 14 months and compared with littermate controls. We found no histologic evidence of PIN or invasive cancer in 18 *TMPRSS2-ERG* mice examined (Fig. 2a). Although mild dysplasia was seen in some transgene-positive mice, these changes are commonly observed in wild-type mice and cannot be definitively attributed to transgene expression.

These data suggest that *TMPRSS2-ERG* is insufficient to initiate prostate neoplasia and that cooperating oncogenic lesions are required. Two relatively common abnormalities in human prostate cancer are *PTEN* loss and *MYC* amplification, both of which play pathogenic roles in genetically engineered mouse models^{5,9}. We therefore examined a cohort of *TMPRSS2-ERG* positive and negative human prostate tumors (n=121) for associated *PTEN* copy number loss or *MYC* amplification as measured by high resolution array-based comparative genome hybridization (aCGH). *TMPRSS2-ERG* status was determined based on interstitial deletion by aCGH and by exon array based mRNA expression profiling, which is highly correlated with fluorescent in situ hybridization analysis¹⁰. Although *PTEN* inactivation can also occur through loss of expression or point mutation, we determined *PTEN* status in these tumors by copy number alteration as this is a common mechanism of *PTEN* loss and provides robust evidence of gene inactivation. Tumors with *PTEN* loss were highly enriched for *ERG* rearrangement (p-value<0.002, Fisher's one-sided exact test, Fig. 2b and Supplementary Tables 1–5), consistent with a similar association between reduced *PTEN* expression (measured by immunohistochemistry) and *ERG* fusion⁸. These studies are meaningful in light of a recent report that concurrent *ERG* rearrangement and *PTEN* loss in human prostate cancers predicts earlier disease recurrence¹¹. In contrast, *c-MYC* amplification was not associated with *ERG* rearrangement (p-value=0.56, Fig. 2c). However,

increased *c-MYC* mRNA levels, as measured by exon array, were associated with *ERG* rearrangement (p-value=0.0465, data not shown), consistent with recent evidence that *c-MYC* is a transcriptional target of *TMPRSS2-ERG*¹². Taken together, these data establish that *PTEN* loss occurs in cooperation with *TMPRSS2-ERG* fusion, however *ERG* rearrangement does not result in selective pressure for *MYC* amplification.

To test the biological significance of the *PTEN/TMPRSS2-ERG* association in human tumors, we crossed our *TMPRSS2-ERG* mice with *Pten* +/- mice⁹. At six months of age, all compound mice examined (8 of 8) showed clear histologic evidence of PIN (Fig 2d). Notably, one *Pten*+/-; *TMPRSS2-ERG* animal had areas suggestive of microinvasive disease with attenuation of the periglandular smooth muscle stroma as well as stromal reaction, and inflammation around affected glands (Fig. 2e, Supplementary Figure 1). A focus of low grade PIN was observed in only 1 out of 8 *Pten* +/- littermate controls where the incidence of PIN at this age is reported to be about 10 percent⁹. To further explore the interaction with the PI3K pathway, we crossed *TMPRSS2-ERG* mice with prostate-specific *AKT* transgenic mice, which develop low grade PIN but do not progress to invasive cancer even at advanced age⁷. In contrast to 8 transgenic *AKT* littermate controls, 8 of 8 bigenic mice examined had developed more florid lesions by 10–12 months of age (Fig. 2f). We also crossed our *TMPRSS2-ERG* mice to *ARR2PB-c-MYC* (Hi-Myc) transgenic mice⁵ and found no evidence of cooperativity in 8 mice at 3 or 6 months, after which nearly all Hi-Myc mice have developed invasive cancer (Supplementary Figure 2). This result is consistent with the failure to detect significant coincidence of *TMPRSS2-ERG* fusion and *c-MYC* amplification in human tumors.

Our finding that *TMPRSS2-ERG* alone is insufficient to induce prostate neoplasia (or PIN) is in agreement with an independent study published in this issue⁸ but contrasts with two other reports that transgenic *ERG* expression induces PIN at 3–6 months of age^{13,14}. These discrepancies are unlikely related to levels of transgene expression. All four models used the *ARR2-Pb* promoter, and our mice express the transgene at levels comparable to Carver et al. (Fig. 1e) and Klezovitch et al. (data not shown). Our mice differ in the inclusion of upstream untranslated *TMPRSS2* sequences in the *ERG* fusion (which may impact translational efficiency, although we have no evidence for this based on transfection experiments) and the use of the variant 2 *ERG* isoform, which is an abundant allele in human tumors. The difference may lie in interpretation of mouse prostate histology, as the changes reported by Klezovitch et al. and by Tomlins et al. are subtle in comparison to the PIN phenotypes seen in other mouse prostate cancer models^{13,14}. The higher frequency of microinvasion in the *ERG*; *Pten* +/- mice in the accompanying report may relate to mouse background because PI3K pathway activation induces a greater degree of proliferation, as measured by Ki-67 staining, in C57BL/6 (Carver et al.) relative to FVB (our model)¹⁵. Collectively, these data establish cooperativity between PI3K pathway activation and *ERG* aberration in induction of PIN but suggest that additional events are likely required for actual malignancy. Comprehensive human prostate cancer oncogenome studies are needed to fully annotate the frequency of alterations in these and other pathways.

Supplementary Material

Refer to Web version on PubMed Central for supplementary material.

Acknowledgments

This work was supported by a Ruth L. Kirschstein NRSA (7F32CA113132) to J.C.K. C.L.S. is an Investigator of the Howard Hughes Medical Institute and a Doris Duke Distinguished Clinical Scholar. B.S.T is a fellow of the Geoffrey Beene Cancer Research Center at MSKCC. We thank Kate Yen, Nicola Clegg, Yu Chen, Tambudzai Shamu, and the MSKCC CMG, Proteomics, and Molecular Cytology Core Facilities for technical help and/or

discussions. We also thank Pier Paolo Pandolfi for sharing unpublished results and Valera Vasioukhin for providing transgenic prostate lobes.

References

1. Kumar-Sinha C, Tomlins SA, Chinnaiyan AM. *Nat Rev Cancer* 2008;8:497–511. [PubMed: 18563191]
2. Perner S, et al. *Am J Surg Pathol* 2007;31:882–888. [PubMed: 17527075]
3. Tomlins SA, et al. *Science* 2005;310:644–648. [PubMed: 16254181]
4. Jhavar S, et al. *J Mol Diagn* 2008;10:50–57. [PubMed: 18165275]
5. Ellwood-Yen K, et al. *Cancer Cell* 2003;4:223–238. [PubMed: 14522256]
6. Zhang J, Thomas TZ, Kasper S, Matusik RJ. *Endocrinology* 2000;141:4698–4710. [PubMed: 11108285]
7. Majumder PK, et al. *Proc Natl Acad Sci U S A* 2003;100:7841–7846. [PubMed: 12799464]
8. Carver BS, et al. *Nat Genet.* 2009 In Press.
9. Di Cristofano A, Pesce B, Cordon-Cardo C, Pandolfi PP. *Nat Genet* 1998;19:348–355. [PubMed: 9697695]
10. Attard G, et al. *Oncogene* 2008;27:253–263. [PubMed: 17637754]
11. Yoshimoto M, et al. *Mod Pathol.* 2008
12. Sun C, et al. *Oncogene* 2008;27:5348–5353. [PubMed: 18542058]
13. Klezovitch O, et al. *Proc Natl Acad Sci U S A* 2008;105:2105–2110. [PubMed: 18245377]
14. Tomlins SA, et al. *Neoplasia* 2008;10:177–188. [PubMed: 18283340]
15. Xu Q, et al. *Proc Natl Acad Sci U S A* 2007;104:17771–17776. [PubMed: 17978178]

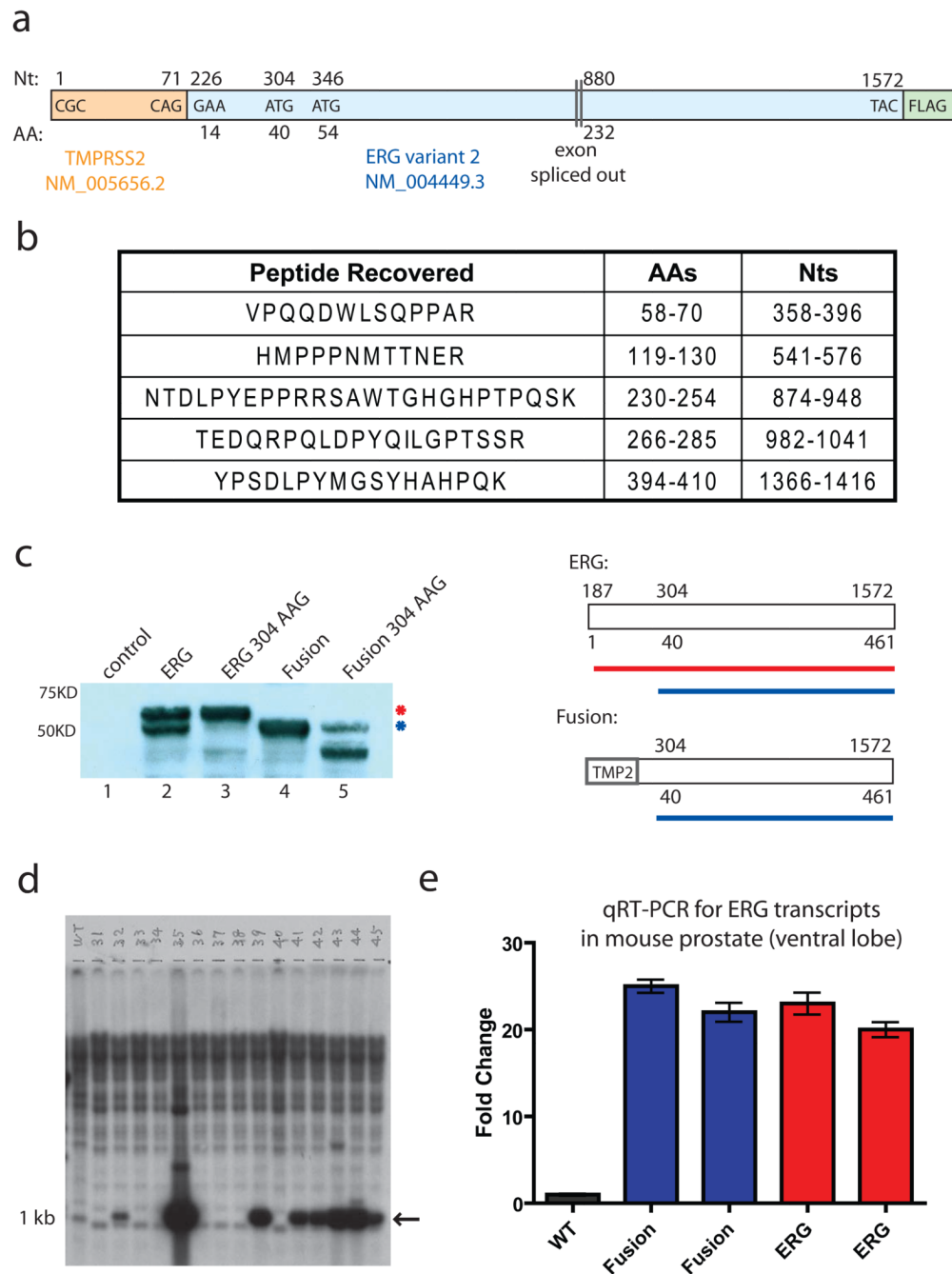
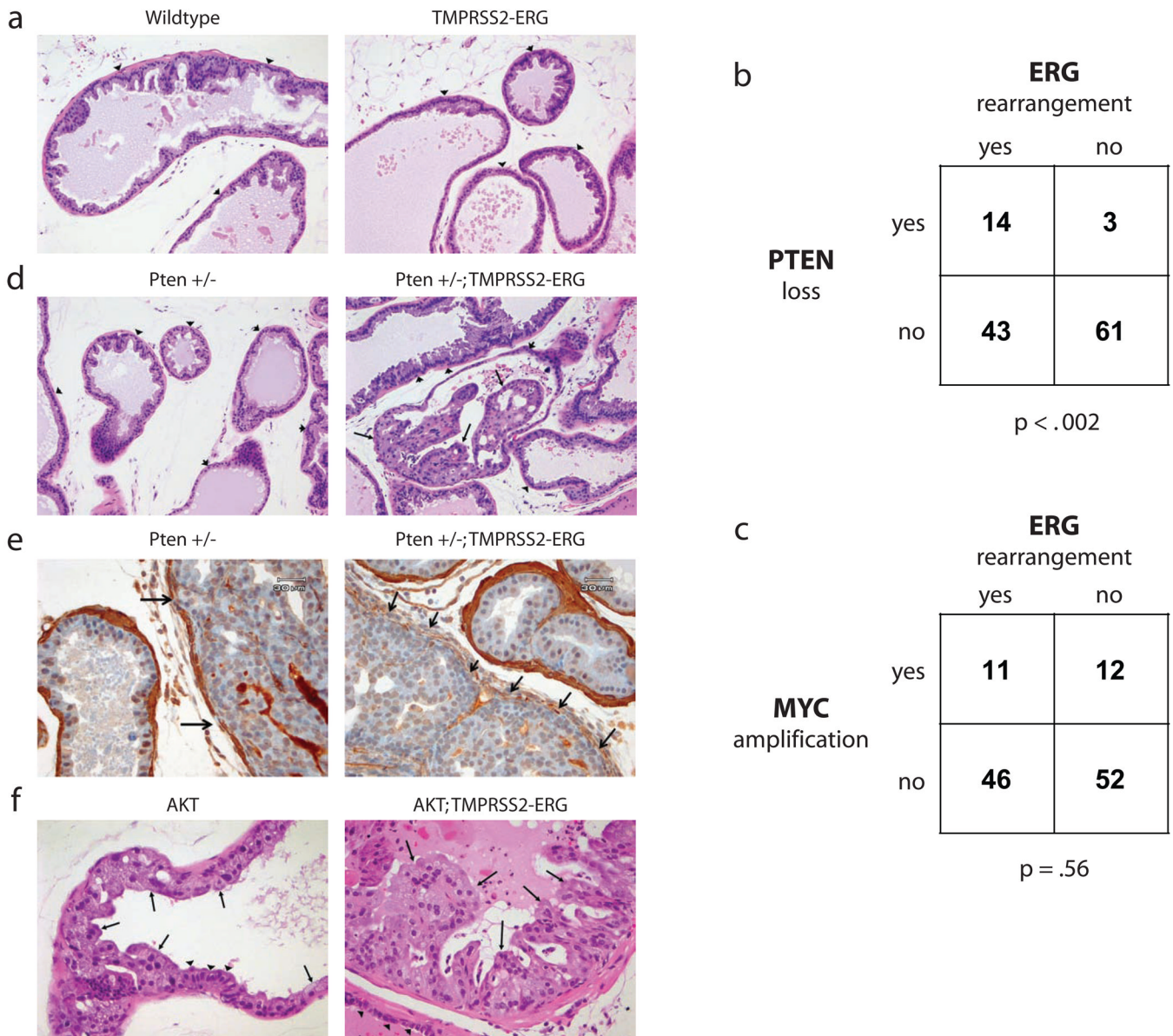


Fig. 1. *TMPRSS2-ERG* fusion transcript produces a truncated ERG protein product. a, Diagram of *TMPRSS2-ERG* variant 2 construct. b, Tryptic peptides recovered from mass spectrometry performed on immunoprecipitated, gel-resolved protein from the fusion construct. c, ERG immunoblot of transiently transfected vector control, full length ERG, full length ERG with codon 304 mutation, fusion, or fusion with the codon 304 mutation. A diagram showing the protein products derived from the non-mutated constructs is shown on the right. d, Southern blot showing founder animals derived from blastocyst injections of *ARR2PB-TMPRSS2-ERG* construct. DNA was cut with BamHI and probed with a BamHI fragment that encodes the first 1050bp of the fusion. e, qRT-PCR using primers for the C-terminus of *ERG* on

ventral prostates from a wildtype mouse, two *TMPRSS2-ERG* mice, and two full-length *ERG* transgenic mice. All Ct values were normalized to the Ct values of *Nkx3.1* and fold change was calculated relative to the wildtype animal.

**Fig. 2.**

TMPRSS2-ERG fusion and PI3K pathway activation are cooperative events in prostate cancer. All pictures show the ventral prostate lobe. a, No PIN is noted in either wild type or *TMPRSS2-ERG* animals at 12 months of age (H&E, 200X). b, The proportion of human prostate cancers that show *PTEN* genomic loss, *ERG* rearrangement, both, or neither are shown ($n = 121$). *PTEN* loss was defined as having reduced copy number by RAE (heterozygous or homozygous loss; FDR q -value $< 6.93 \times 10^{-8}$). *ERG* rearrangement was defined as the consequence of interstitial deletion by aCGH (q -value $< 6.93 \times 10^{-8}$) and increased expression of *ERG* downstream of common translocation breakpoints (exons 5–8) relative to early *ERG* exons (exons 1–2) [> 2 s.d. above the mean of normal samples ($n=29$) by exon expression array] The significance of the association between *PTEN* loss and *ERG* rearrangement is p -value < 0.002 as determined by Fisher's exact test (right tail). c, The proportion of human prostate cancers that show *MYC* genomic amplification, *ERG* rearrangement, both, or neither are shown ($n = 121$). *MYC* amplification was defined as

having increased copy number ($q\text{-value} < 1.2 \times 10^{-7}$). *ERG* rearrangement and the significance of association ($p\text{-value} = 0.56$) was defined as in Fig 2b. d, Normal prostate in *Pten* +/- and high grade PIN in *Pten* +/-; *TMPRSS2-ERG* mice at 6 months of age (H&E, 200X). Arrows indicate PIN and arrowheads show normal epithelium for comparison. e, Immunohistochemistry for smooth muscle actin in a *Pten* +/- and a *Pten* +/-; *TMPRSS2-ERG* mouse (400X). Compare disrupted and absent smooth muscle stroma around areas of possible microinvasion from a *Pten* +/-; *TMPRSS2-ERG* mouse (right column, arrows) to minimally attenuated smooth muscle sheath around area of high grade PIN in *Pten* +/- (left column, arrows) and to intact stroma of normal glands in both animals. f, Low grade PIN in *AKT* transgenic mice and high grade PIN in *AKT*; *TMPRSS2-ERG* double transgenic animals at 11 months of age (H&E, 400X). Arrows indicate PIN and arrowheads show normal epithelium for comparison.